Mother wavelet functions generalized through q-exponentials

Mother wavelet functions generalized through q-exponentials

Ernesto P Borges[1,2]**, Constantino Tsallis**[2,3]**, José G V Miranda**[4]
and Roberto F S Andrade[4]

[1] Escola Politécnica, Universidade Federal da Bahia, R. Aristides Novis, 2, 40210-630 Salvador, BA, Brazil
[2] Centro Brasileiro de Pesquisas Físicas, R Dr Xavier Sigaud 150, 22290-180 Rio de Janeiro, RJ, Brazil
[3] Santa Fe Institute, 1399 Hyde Park Road, Santa Fe, NM, 87501, USA
[4] Instituto de Física, Universidade Federal da Bahia, Campus Universitário de Ondina, 40210-340 Salvador, BA, Brazil

E-mail: ernesto@ufba.br, tsallis@cbpf.br, vivas@ufba.br and randrade@ufba.br

Abstract
We generalize some widely used mother wavelets by means of the q-exponential function $\mathrm{e}_q^x \equiv [1 + (1 - q)x]^{1/(1-q)}$ $\left(q \in \mathbb{R}, \mathrm{e}_1^x = \mathrm{e}^x\right)$ that emerges from nonextensive statistical mechanics. In particular, we define extended versions of the Mexican hat and the Morlet wavelets. We also introduce new wavelets that are q-generalizations of the trigonometric functions. All cases reduce to the usual ones as $q \to 1$. Within nonextensive statistical mechanics, departures from unity of the entropic index q are expected in the presence of long-range interactions, long-term memory, multi-fractal structures, among others. Consistently the analysis of signals associated with such features is hopefully improved by proper tuning of the value of q. We exemplify with the wavelet transform modulus-maxima method for mono- and multi-fractal self-affine signals.

PACS numbers: 02.30.−f, 02.30.Nw, 05.20.−y, 05.45.Tp

1. Introduction

The basic idea behind the analysis of a temporal or spatial signal by a Fourier transform is *similarity*. For instance, the inner product $\langle \phi_n(x), f(x) \rangle$ expresses how similar are the function $f(x)$ and the nth element of the basis $\{\phi_n(x)\}$ (the kernel of the transform). The kernel of Fourier transform is a plane wave and here lies its simplicity, but also its limitation. Rigorously speaking, a plane wave exists everywhere in the universe and at all (past and future) times.

Hence there are no plane waves in nature. All physical signals are temporary and spatially limited. As a consequence of the infinitely extended kernel, the Fourier transform is unable to satisfactorily determine *when* a burst has occurred, or *where* edges of images are located, for example (the Gibbs phenomenon, see, for instance, [1, 2]).

The first attempt to overcome limitations of Fourier analysis was that of Gabor [3], who introduced a windowed Fourier transform [4]. He used a modulation function $g(u - t)$ in order to localize the signal in a time interval $[t - T, t]$ (supp $g \subset [-T, 0]$). Translations in time would cover the whole signal. With this, he achieved time-frequency localization. But a problem still remains with the use of a fixed scale window: signal details much smaller than the window width T are detected, but not localized. They appear in the frequency behaviour of the windowed Fourier transform in a similar way it would appear in the usual Fourier transform. Signal features much larger than T, on the other hand, appear in the time behaviour of the windowed Fourier transform (i.e., they are not detected).

To avoid this problem, it is sufficient to scale a free transform. Wavelet analysis was developed to accomplish this goal. The windowed Fourier transform uses a fixed size window and fills it with oscillations of different frequencies (consequently, varies the number of oscillations within the window). The wavelet transform uses a function with fixed number of oscillations and varies the width of the window. Dilations and translations generate a complete analysis of the signal. This procedure automatically uses small windows to identify high-frequency components of a signal, and large windows for low-frequency components. Wavelet analysis provides a time-scale (instead of a time-frequency) localization.

Wavelet analysis was developed more than a century and a half after the pioneering work of Fourier [5]. Since the 1980s it has grown so fast that it has already consolidated as a field of research of its own.

Another emerging science is nonextensive statistical mechanics, that also began in the 1980s, with the formulation of the concept of a nonextensive entropy [6] that generalizes the Boltzmann–Gibbs entropy, as a basis of a generalization of standard statistical mechanics itself. Here, it took also more than a century since the first formulation of the concept of entropy. Nonextensive statistical mechanics [6–9] seems to give an underlying formal basis for a variety of complex phenomena, such as anomalous diffusion [10–16], self-gravitating systems [17, 18], turbulence [19–25], cosmic rays [26, 27], among others (for an updated bibliography, see [28]).

The definition of the nonextensive q-entropy [6] is

$$S_q \equiv k \frac{1 - \sum_{i=1}^{W} p_i^q}{q - 1} \quad (k > 0). \tag{1}$$

The entropic index q characterizes the generalization and the Boltzmann–Gibbs–Shanon entropy, $S_1 = -k \sum_i p_i \ln p_i$, is recovered at $q \to 1$. The canonical ensemble is obtained by maximizing (1) with the norm constraint $\left(\sum_{i=1}^{W} p_i = 1 \right)$ and also imposing the constancy of the normalized q-expectation value of the energy [29]

$$U_q = \sum_{i=1}^{W} \epsilon_i P_i^{(q)}, \tag{2}$$

where $\{\epsilon_i\}_{i=1}^{W}$ are the eigenvalues of the Hamiltonian of the system, and $\left\{ P_i^{(q)} \right\}_{i=1}^{W}$ are the escort probabilities, defined by [30]

$$P_i^{(q)} \equiv \frac{p_i^q}{\sum_{j=1}^{W} p_j^q}, \tag{3}$$

with p_i being the probability associated with the ith state, given by

$$p_i = \frac{[1 - (1-q)\beta'\epsilon_i]^{\frac{1}{1-q}}}{Z'_q}. \tag{4}$$

If $q < 1$, $p_i \equiv 0$ whenever $[1 - (1-q)\beta'\epsilon_i] \leqslant 0$ (cut-off condition). The partition function Z'_q is defined as

$$Z'_q \equiv \sum_{j=1}^{W}[1 - (1-q)\beta'\epsilon_j]^{\frac{1}{1-q}} \tag{5}$$

and

$$\beta' = \frac{\beta}{\sum_{j=1}^{W} p_j^q + (1-q)\beta U_q}, \tag{6}$$

where β is the Lagrange parameter associated with the constraint (2). The striking features of (4) are its power law for $q > 1$, and the cut-off for $q < 1$, which generates quite different behaviours when compared with the Boltzmann–Gibbs exponential distribution. The meaning of the word *nonextensive* can be easily understood if we consider a system composed of two independent subsystems (in the sense of probability theory, $p_{ij}^{(A+B)} = p_i^{(A)} p_j^{(B)}$). According to (1), the q-entropy of the composite system is given by

$$S_q^{(A+B)} = S_q^{(A)} + S_q^{(B)} + (1-q)S_q^{(A)} S_q^{(B)}. \tag{7}$$

Clearly $q \neq 1$ yields nonadditivity, or nonextensivity. A system with $q > 1$ is said to be subadditive, and if $q < 1$, it is superadditive.

The functional forms of (1) and (4) inspired the definition of generalizations of the logarithm and exponential functions [31, 32]:

$$\ln_q x \equiv \frac{x^{1-q} - 1}{1 - q}, \tag{8}$$

$$e_q^x \equiv \begin{cases} [1 + (1-q)x]^{\frac{1}{1-q}}, & \text{if } [1 + (1-q)x] > 0 \\ 0, & \text{otherwise.} \end{cases} \tag{9}$$

It follows immediately that $\ln_q\left(e_q^x\right) = e_q^{\ln_q(x)} = x$. The original logarithm and exponential functions are recovered as the particular cases $\ln_1 x$ and e_1^x. Many formal developments have been made concerning such functions. Among them we point out the generalization [33] of the celebrated Shannon's theorem. Obviously there are infinitely many ways of generalizing a given function. One common form of generalizing the exponential is $\exp_q(x) \equiv \sum_n x^n / (n)_q!$, with $(n)_q! = \prod_{j=1}^{n}(j)_q$ and $(j)_q = (q^j - 1)/(q - 1)$ and also $(0)_q! = 1$. This particular expression has applications in quantum groups [34]. In this paper we will not explore this possibility, but rather the one given by equation (9) above, that naturally emerges from nonextensive statistical mechanics. Relations between wavelet analysis and nonextensive statistical mechanics have already been reported, including applications in biophysics, as the analysis of EEG signals [35–39].

The purpose of this paper is to extend the use of such q-deformed functions into wavelet analysis by generalizing some widely used wavelet functions. In particular, we generalize the Mexican hat (section 2) and the modulated Gaussian (section 3). Moreover, we introduce in section 4 a pair of even and odd wavelets based on the generalization of trigonometric functions. Finally (section 5) we exemplify, with the wavelet transform modulus-maxima method (WTMMM) for mono- and multi-fractal self-affine signals, the possible use of the introduced functions and, lastly, we present our final remarks (section 6).

2. *q*-Mexican hat

Before we discuss the properties of the wavelets based on definitions (8) and (9), let us indicate some basic facts about continuous *g*-wavelet transform of a function f, $T_g(a, b)f$, which is defined by

$$T_g(a, b)f = a^{-1/2}C_g^{-1/2}\int_{-\infty}^{\infty} dx\, f(x)g\left(\frac{x-b}{a}\right). \tag{10}$$

In order that a given function $g \in L^2(\mathbb{R})$ can be considered as a mother wavelet, it must satisfy the so-called admissibility condition, that can be expressed in terms of its Fourier transform $\hat{g}(\omega)$ by

$$C_g = 2\pi \int_{-\infty}^{\infty} d\omega |\hat{g}(\omega)|^2/|\omega| < \infty. \tag{11}$$

It essentially means that $g(x)$ has zero mean, i.e.,

$$\int_{-\infty}^{\infty} dx\, g(x) = 0 \tag{12}$$

and ensures that the original function $f(x)$ can be recovered from its wavelet transform as

$$f(x) = C_g^{-1/2} \int_{-\infty}^{\infty} db \int_0^{\infty} da \frac{1}{a^2} T_g(a, b)fg\left(\frac{x-b}{a}\right). \tag{13}$$

This expression shows that, if a mother wavelet g satisfies (11), it generates, by its translations and dilations, a basis in the Hilbert space, so that any function $f \in L^2(\mathbb{R})$ can be expressed in terms of its *g*-wavelet components. It is well known that orthonormal wavelet bases can only be defined within the discrete formulation, i.e., when $b \in \mathbb{Z}$ and $a = a_0^j$, with $a_0 > 0$ and $j \in \mathbb{Z}$. So, orthonormal bases cannot be defined with the help of the functions we discuss below.

A simple and quite common example of continuous wavelet is the Mexican hat (see, for instance, [40–42]) that is generated from the Gaussian distribution

$$\begin{aligned}\psi(x) &= -A\frac{d^2\, e^{-x^2/2}}{dx^2}, \\ &= A(1-x^2)\, e^{-x^2/2}.\end{aligned} \tag{14}$$

The normalization constant is given by $A = 2/(\pi^{1/4}\sqrt{3})$. Generalization of Gaussian distribution within nonextensive scenario we are focusing here has already been made [15, 16]. The *q*-Gaussian $\left(\propto e_q^{-\beta x^2}\right)$ unifies a great variety of different distributions into a single family, parametrized by q (see [15, 16] for details): Gaussian distribution is recovered, of course, for $q = 1$. Moreover, for $q = 2$, we have the Cauchy–Lorentz distribution. Besides, $q \to 3$ yields a completely flat distribution, and $q \to -\infty$ yields Dirac's δ. This unifying character of the *q*-Gaussian, as well as its empirically observed occurrence in a variety of complex phenomena (as cited in introduction) stimulate us to explore its potential use in wavelet analysis. One of the more simple applications that immediately come to mind is to use it in order to generalize the Mexican hat, a function that is proportional to the second derivative of a Gaussian. We could simply replace an ordinary Gaussian by a *q*-Gaussian, which is a legitimate choice. Instead of doing that, we prefer to adopt a variation of it, and take the second derivative of a *power* of a *q*-Gaussian, according to the recipe

$$\psi_q(x) \propto \frac{d^2\left[e_q^{-\beta x^2}\right]^{2-q}}{dx^2}, \tag{15}$$

which yields the expression for the q-Mexican hat

$$\psi_q(x) = A_q[1 - (3 - q)\beta x^2]\left[e_q^{-\beta x^2}\right]^q. \tag{16}$$

With this choice we arrive, according to the expression above, at a q-Gaussian raised to the power q, resembling the escort probabilities, equation (3), widely used in nonextensive formalism [29]. We call the attention of the reader to the fact that $\left[e_q^a\right]^b \neq \left[e_q^{ab}\right]$, except, of course, in the particular case $q = 1$. Because of this, the semigroup property is not satisfied, but it is exactly this that generates its nonextensive behaviour equation (7). For some properties of the q-exponential and the q-logarithm, see [43–47].

If $-1 < q < 1$ and $|x| = [(1-q)\beta]^{-1/2}$, the cut-off of the q-exponential (see equation (9)) imposes $\psi_q(x) = 0$. It is easily proved that, for $-1 < q < 3$, equation (11) holds, so that any $\psi_q(x)$ is a well-defined mother wavelet. For $q \leqslant -1$ or $q \geqslant 3$, $\psi_q(x)$ does not satisfy the admissibility condition and cannot be used to define a useful mother wavelet.

The normalization constant is given by

$$A_q = \frac{\beta^{1/4}}{\pi^{1/4}\sqrt{3}}\left[\frac{(q - 1)^{5/2}\Gamma\left(\frac{2q}{q-1}\right)}{\Gamma\left(\frac{2q}{q-1} - \frac{5}{2}\right)}\right]^{1/2} \tag{17}$$

if $1 < q < 3$, and

$$A_q = \frac{\beta^{1/4}}{\pi^{1/4}\sqrt{3}}\frac{(5 - q)^{1/2}(3 + q)^{1/2}}{2}\left[\frac{(1 - q)^{1/2}\Gamma\left(\frac{2q}{1-q} + \frac{3}{2}\right)}{\Gamma\left(\frac{2q}{1-q} + 1\right)}\right]^{1/2} \tag{18}$$

if $-1 < q < 1$.

The function $\psi_q(x)$ satisfies the admissibility condition and consistently recovers the Mexican hat, $\lim_{q \to 1} \psi_q(x) = \psi_1(x)$. The range of admissible values for $q(-1 < q < 3)$ is divided in three regions. For $1 < q < 3$, $\psi_q(x)$ is infinitely supported and presents a power-law tail $\sim -1/|x|^{2/(q-1)}$, in marked contrast to the exponential tail of the original Mexican hat. When $q < 1$, a cut-off naturally appears at $|x_c| = [(1 - q)\beta]^{-1/2}$. In the range $0 < q < 1$, $\psi_q(x_c) = 0$, and when $-1 < q < 0$, $\psi_q(x_c)$ diverges. For $q \to -1$, $\psi_q(x)$ coincides with the abscissa axis, except at the cut-off positions, where it diverges. These features introduce significant differences from the original Mexican hat wavelet. Figure 1 illustrates $\psi_q(x)$ with $\beta = 1/2$.

The Fourier transform,

$$\mathcal{F}[f(x); y] \equiv F(y) \equiv \frac{1}{\sqrt{2\pi}}\int_{-\infty}^{\infty} e^{ixy} f(x)\, dx, \tag{19}$$

of $\psi_q(x)$ may be found by considering (15), and taking into account the property of the Fourier transform of derivatives, $\mathcal{F}[f^{(n)}; y] = (-iy)^n F(y)$, together with the Fourier transform of a q-Gaussian (see equations (3.384 9) and (3.387 2) of [48]). We find for $1 < q < 3$,

$$\mathcal{F}[\psi_q(x); y] = \frac{A_q}{(2 - q)\beta}\frac{1}{\sqrt{2(q-1)\beta}\Gamma\left(\frac{2-q}{q-1}\right)}y^2\left[\frac{|y|}{2\sqrt{(q-1)\beta}}\right]^{\nu}K_\nu\left(\frac{|y|}{\sqrt{(q-1)\beta}}\right), \tag{20}$$

and for $-1 < q < 1$,

$$\mathcal{F}[\psi_q(x); y] = \frac{A_q}{2(2 - q)\beta}\frac{\Gamma\left(\frac{2-q}{1-q} + 1\right)}{\sqrt{2(1-q)\beta}}y^2\left[\frac{2\sqrt{(1-q)\beta}}{y}\right]^{-\nu}J_{-\nu}\left(\frac{y}{\sqrt{(1-q)\beta}}\right), \tag{21}$$

with $\nu = \frac{2-q}{q-1} - \frac{1}{2}$. $J_{-\nu}$ is the Bessel functions of the first kind and K_ν is the modified Bessel function of the second kind.
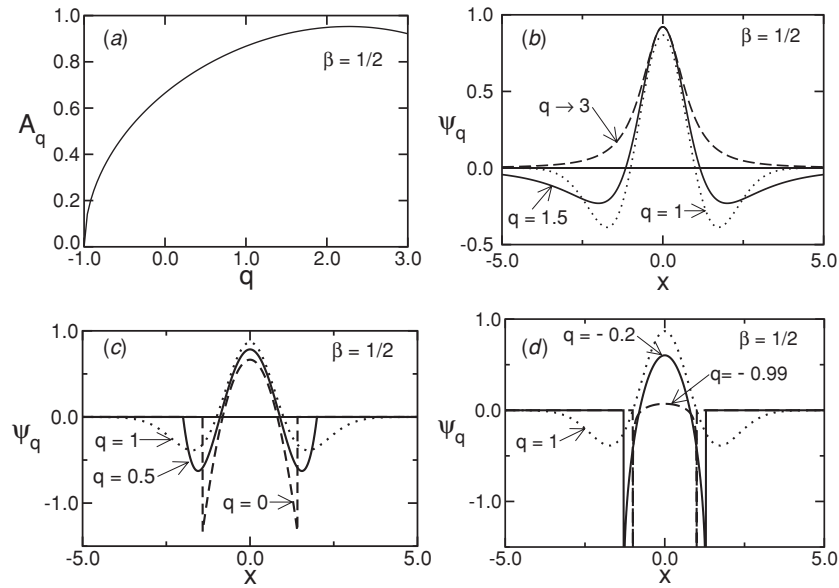
Figure 1. q-Mexican hat with $\beta = 1/2$. (a) Normalization constant A_q, (b) $\psi_q(x)$ for $1 < q < 3$, (c) $0 < q < 1$, (d) $-1 < q < 0$. The usual Mexican hat ($q = 1$) is represented by a dotted line, for comparison.

It is possible to have variations of the q-Mexican hat by using $\beta = \beta(q)$ (with $\beta(1) = \frac{1}{2}$), for instance, $\beta = 1/(3-q)$.

3. Modulated q-Gaussian

Now we turn to the Morlet wavelet, or modulated Gaussian [49–51], a function associated with the birth of wavelet analysis [52, 53]. Within the context we are dealing with, we search for a wavelet that is a generalization of [40, 54]

$$h(x) = \pi^{-1/4}(e^{-ikx} - e^{-k^2/2}) e^{-x^2/2}, \tag{22}$$

where $k = \pi(2/\ln 2)^{1/2}$. So we simply modulate the usual trigonometric functions ($e^{-ik_q x}$) with a q-Gaussian $\left(e_q^{-\beta x^2}\right)$:

$$h_q(x) = B_q(e^{-ik_q x} - \Lambda_q(k_q)) e_q^{-\beta x^2}, \qquad \infty < q < 3. \tag{23}$$

The function $\Lambda_q(k_q)$ is such that the admissibility condition, written in the domain of frequencies,

$$\mathcal{F}[h_q(x); 0] = 0, \tag{24}$$

is satisfied. It means that

$$\Lambda_q(k_q) \equiv \frac{\mathcal{F}\left[e^{-ik_q x} e_q^{-\beta x^2}; 0\right]}{\mathcal{F}\left[e_q^{-\beta x^2}; 0\right]}. \tag{25}$$

Taking into account the Fourier transform of a q-Gaussian (see equations (3.384 9) and (3.387 2) of [48]), and $\mathcal{F}[e^{-ik_q x}; y] = \sqrt{2\pi}\delta(y - k_q)$, and also, from the convolution theorem

(with the symmetric convention (19) we are adopting here),

$$\mathcal{F}[f(x)g(x); y] = F(y) * G(y)$$
$$= \frac{1}{\sqrt{2\pi}} \int_{-\infty}^{\infty} F(y - \xi)G(\xi) \, d\xi, \tag{26}$$

we find for $q > 1$,

$$\Lambda_q(k_q) = \frac{2}{\Gamma\left(\frac{1}{q-1} - \frac{1}{2}\right)} \left(\frac{k_q}{2\sqrt{(q-1)\beta}}\right)^{\mu} K_{\mu}\left(\frac{k_q}{\sqrt{(q-1)\beta}}\right), \tag{27}$$

and for $q < 1$,

$$\Lambda_q(k_q) = \Gamma\left(\frac{1}{1-q} + \frac{3}{2}\right) \left(\frac{2\sqrt{(1-q)\beta}}{k_q}\right)^{-\mu} J_{-\mu}\left(\frac{k_q}{\sqrt{(1-q)\beta}}\right), \tag{28}$$

with $\mu = \frac{1}{q-1} - \frac{1}{2}$. We follow the same criterion adopted by [40] for the determination of the value of k_q: the ratio between the second highest and highest local maxima of Re h_q is $1/2$. It results that

$$k_q = 2\pi\sqrt{\frac{(q-1)\beta}{2^{q-1} - 1}} \qquad (q \gtrless 1). \tag{29}$$

The normalization constant B_q is given by

$$B_q = \begin{cases} \left(\frac{\beta}{\pi}\right)^{1/4} \left[\frac{(q-1)^{1/2}\Gamma\left(\frac{2}{q-1}\right)}{\Gamma\left(\frac{2}{q-1} - \frac{1}{2}\right)}\right]^{1/2}, & 1 < q < 3, \\ \\ \left(\frac{\beta}{\pi}\right)^{1/4} \left[\frac{(1-q)^{1/2}\Gamma\left(\frac{2}{1-q} + \frac{3}{2}\right)}{\Gamma\left(\frac{2}{1-q} + 1\right)}\right]^{1/2}, & q < 1. \end{cases} \tag{30}$$

(B_q is an approximation, as $B_1 = \pi^{-1/4}$ of equation (22) is also an approximation.) Figure 2 illustrates $\sqrt{2}$ Re h_q with $\beta(q) = 1/(3 - q)$. (The factor $\sqrt{2}$ is used to have the real part normalized.) We observe the long (power-law) tail for $1 < q < 3$, in marked contrast to the rapidly vanishing tail for $q = 1$. The cut-off is present for $q < 1$. In the case $q \rightarrow -\infty$, $h_q(x)$ reduces to a two-cycle function, the imaginary part of it is a variation of the one-cycle sine presented in [40].

4. q-trigonometric wavelets

The q-exponential function (9), expanded to the imaginary (or, more generally, complex) domain by analytic continuation, leads to q-trigonometric functions [32]:

$$\cos_q x = \frac{e_q^{ix} + e_q^{-ix}}{2}, \qquad \sin_q x = \frac{e_q^{ix} - e_q^{-ix}}{2i}. \tag{31}$$

The q-cosine and q-sine functions may be expressed as $e_q^{ix} = \rho_q(x) \, e^{i\varphi_q(x)}$ where

$$\rho_q^2(x) = e_q^{(1-q)x^2}, \qquad \varphi_q(x) = \frac{\arctan_1[(1-q)x]}{1-q}. \tag{32}$$

We want to construct a wavelet based on such q-trigonometric functions. For this purpose, we recall that the derivative of a q-exponential may be expressed as
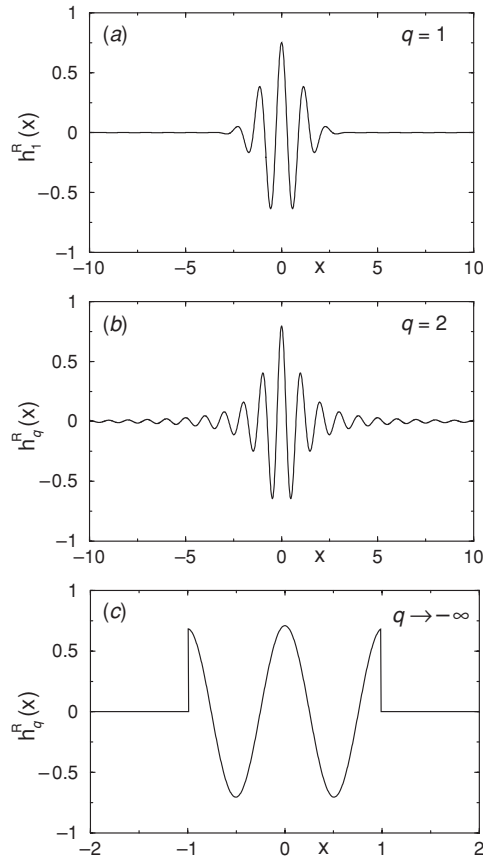
$$\frac{de_q^x}{dx} = e_{2-1/q}^{qx}. \tag{33}$$

Figure 2. Normalized real part of the q-modulated Gaussian ($h_q^R(x) \equiv \sqrt{2}\, \text{Re}\, h_q$). (*a*) $q = 1$ (usual case), (*b*) $q = 2$, (*c*) $q \to -\infty$ (illustrated with $q = -100$). Note that the abscissa scale in (*c*) is different from the others.

Once $\rho_{q>1}(x) \to 0$ for $|x| \to \infty$, the admissibility condition is satisfied for $1 < q < 2$. Renaming the parameter q, we define the following q-trigonometric wavelet:

$$\text{wt}_q(x) \equiv C_q\, e_q^{\frac{ix}{2-q}}, \qquad 1 < q < 2. \tag{34}$$

The normalization constant is given by

$$C_q = \sqrt{\frac{1}{2-q}} \frac{1}{\pi^{1/4}} \left[\frac{(q-1)\Gamma\left(\frac{1}{q-1}\right)}{\Gamma\left(\frac{1}{q-1} - \frac{1}{2}\right)} \right]^{1/2}. \tag{35}$$

For brevity of notation, we can write the real and imaginary parts of $\text{wt}_q(x)$ as

$$\text{wc}_q(x) \equiv \sqrt{2}\, \text{Re}\, \text{wt}_q(x) = \sqrt{2} C_q \cos_q\left(\frac{x}{2-q}\right), \tag{36}$$

$$\text{ws}_q(x) \equiv \sqrt{2}\, \text{Im}\, \text{wt}_q(x) = \sqrt{2} C_q \sin_q\left(\frac{x}{2-q}\right). \tag{37}$$

Some typical curves are shown in figure 3 (for brevity, we only show the odd function $\text{ws}_q(x)$). Note that the number of oscillations decreases as q goes from 1 to 2. The functions
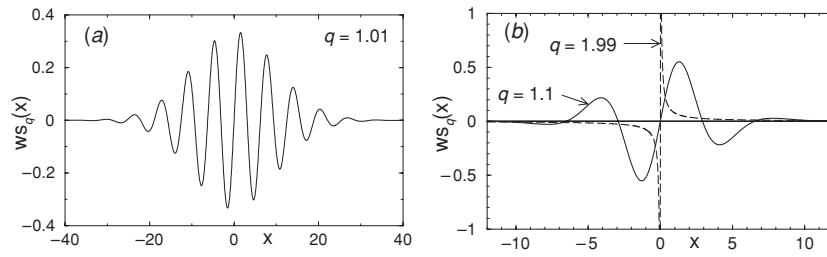
Figure 3. $\mathrm{ws}_q(x)$ versus x. (a) $q = 1.01$, (b) $q = 1.1$ (solid) and $q = 1.99$ (dashed).

present infinite oscillations of vanishing amplitudes at $q \to 1(C_{q\to1} \to 0)$. $\mathrm{ws}_q(x)$ presents only one root, at $x_0 = 0$, for $\frac{3}{2} \leqslant q < 2$, and $\mathrm{wc}_q(x)$ presents only one pair of roots, at $x_0 = \pm\frac{2-q}{q-1}\tan\left[(q-1)\frac{\pi}{2}\right]$, for $\frac{4}{3} \leqslant q < 2$. As $q \to 2, C_q \to \infty$, and the wavelets become sharply localized (the roots of $\mathrm{wc}_q(x)$ approaches $\pm 2/\pi$). Let us also mention that the modulation of the functions is not Gaussian, but rather a power-law decay. But they are essentially different from the modulated q-Gaussian derived in the previous section.

The Fourier transform of $\mathrm{wc}_q(x)$ and $\mathrm{ws}_q(x)$ is found with equation (31) and (see equations (3.382 6) and (3.382 7) of [48])

$$\mathcal{F}\left[\mathrm{e}_{q>1}^{\mathrm{i}ax}; y\right] = \begin{cases} 0, & y > 0, \\[2mm] \dfrac{\sqrt{2\pi}\,(-y)^{\frac{1}{q-1}-1}\,\mathrm{e}^{\frac{y}{(q-1)a}}}{[(q-1)a]^{\frac{1}{q-1}}\,\Gamma\left(\frac{1}{q-1}\right)}, & y < 0, \end{cases} \tag{38}$$

and

$$\mathcal{F}\left[\mathrm{e}_{q>1}^{-\mathrm{i}ax}; y\right] = \begin{cases} \dfrac{\sqrt{2\pi}\,y^{\frac{1}{q-1}-1}\,\mathrm{e}^{\frac{-y}{(q-1)a}}}{[(q-1)a]^{\frac{1}{q-1}}\,\Gamma\left(\frac{1}{q-1}\right)}, & y > 0, \\[2mm] 0, & y < 0. \end{cases} \tag{39}$$

5. An example

Wavelet transforms constitute a multi-purpose tool that rapidly met widespread applications in many areas of pure and applied sciences. To exemplarily demonstrate the reliability of q-wavelets, we briefly present how they can be used to reproduce several properties of well-known fractal sets.

Consider a self-affine profile $y = f_*(x)$ shown in figure 4. Its construction starts with the generator shown in the inset. The generator is recursively applied for each straight line segment. The self-affine fractal profile is obtained in the limit of infinite iterations.

The resulting figure after infinite generations has a local fractal dimension $D = 2 - \alpha$, where $\alpha = \ln B_y/\ln B_x = 0.5$ is the roughness exponent, and B_x and B_y are the scaling factors along the x and y axis, respectively. To analyse the scaling properties of $f(x)$ around an arbitrary point x_0, we shift the origin and define

$$f_{x_0}(x) = f(x_0 + x) - f(x_0) \approx Ax^{\alpha(x_0)} \tag{40}$$

where $\alpha(x_0)$, the Holder (or singularity) exponent of $f_{x_0}(x)$, indicates how this function vanishes (or diverges) at $x = x_0$.

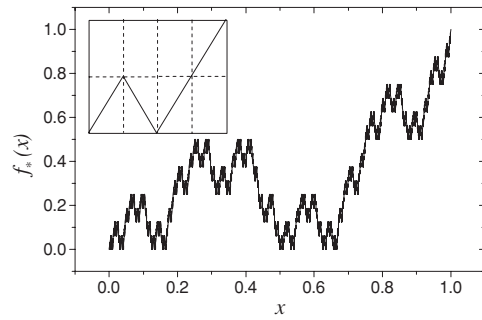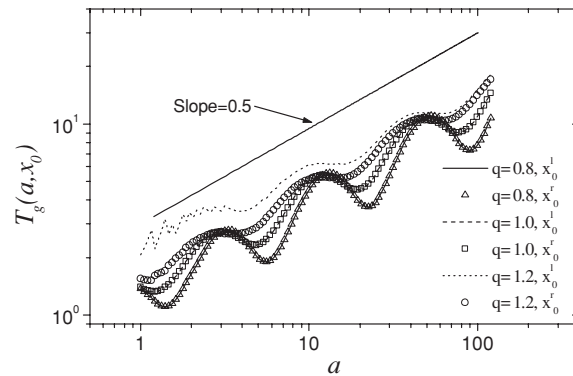**Figure 4.** Self-affine monofractal profile. Inset: its generator.

Figure 5. Wavelet transform (equation (41)) with two different values of b: $x_0^l = 0.25$ and $x_0^r = 0.50$. Note that the curves for the same values of q coincide, as it should be for a monofractal.

Using a general wavelet transform of $f_{x_0}(x)$, it is straightforward to show that the Holder exponent follows immediately from the wavelet transform as

$$T_g(a, b) f_{x_0}(x) \sim a^{\alpha(x_0)}. \tag{41}$$

Figure 5 shows how the q-wavelet transform (equation (41)) behaves for two points along the profile for some values of q. The curves clearly indicate that the value $\alpha = 0.5$ is accurately reproduced. We observe that the results for $q > 1$ show small irregularities. This is due to the fact that, as e_q^{-x} decays only as a power law when $x \to \infty$, the numerical integration in (41) must be performed over a wider interval than for $q \leqslant 1$. In order to make evident this effect, we have performed all integrals over a fixed integration interval. On the other hand, results for $q < 1$ show good convergence, as the function naturally presents a cut-off. Oscillations in the curves are typical for this kind of analysis, as shown in the same figure for the usual Mexican hat ($q = 1$).

Results for a more complex situation can be explored if we consider a multi-fractal set. It is generated along a similar way used to obtain the first set, where we choose two different scaling factors for the first and second half of the profile in each generation of its construction. The plots for different values of x_0 have different slopes (figure 6), indicating that many scaling laws and fractal dimensions are found in the resulting profile.

q-wavelets also prove to be a reliable tool for analysing this much more complex situation that requires a multi-fractal formalism. This amounts to evaluate the generalized fractal dimensions D_Q, or its Legendre transformed singularity spectrum $f(\alpha) = \tau(q) - \alpha Q$,
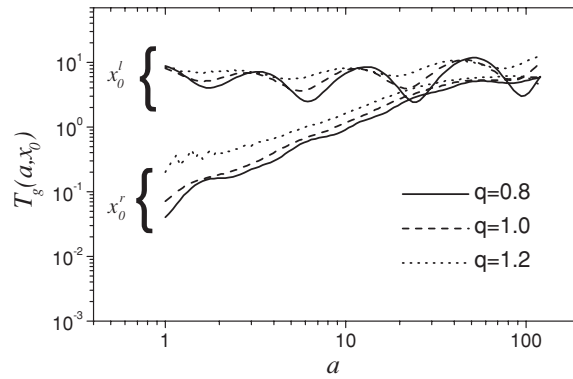
Figure 6. Wavelet transform (equation (41)) with two different values of b: $x_0^l = 0.25$ (upper curves) and $x_0^r = 0.75$ (lower curves). The slopes are clearly different, as a signature of the multi-fractal nature.
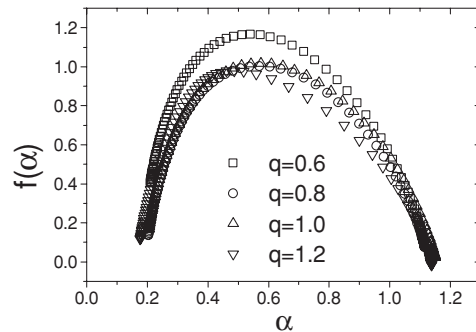

Figure 7. $f(\alpha)$ spectra for the multi-fractal profile. For $q = 0.8$ results are very similar to those with $q = 1$. $q = 0.6$ yields spurious results.

where α represents the Holder exponent. This analysis proceeds within the so-called wavelet transform modulus-maxima method that has been developed in recent years. We will not show the details, which can be found, e.g., in [55].

Figure 7 shows the $f(\alpha)$ spectra, for different values of q, corresponding to the multi-fractal profile. The graphs indicate that the spectra produced by q-wavelets, with $q < 1$, are comparable to that obtained by the usual $q = 1$ Mexican hat. As we fixed the integration interval for all values of q, we observe major differences in the spectra for values $q > 1$. This limitation to its practical use is expressed by larger numerical effort to compute the integrals in the wavelet transforms with the same accuracy for values of $q \leqslant 1$.

6. Final remarks

The functions here introduced generalize widely used mother wavelet functions by means of a single parameter. The q-wavelets present significant different behaviours, when compared with the original $q = 1$ cases. The fingerprints of the generalized q-wavelets are the power-law decay ($q > 1$), and the cut-off ($q < 1$). The generalization was inspired in the nonextensive statistical mechanics and the q-exponential that emerges from it. Within this formalism, the entropic index q measures departures from the usual Boltzmann–Gibbs behaviour. There is a

number of possible origins for such departures, such as slow (power-law) mixing, long-range (spatial) interactions, long-term (temporal) memory or fractal nature of the phase space. When dealing with signals which exhibit some of these features, one can hopefully take advantage of the index q to tune the wavelet to the signal, as is here briefly exemplified for the q-Mexican hat. Other wavelets, as well as scaling functions, may be generalized along the lines here introduced, for instance, the Meyer wavelet or the sinc function.

Acknowledgments

References

[1] Kreyszig E 1993 *Advanced Engineering Mathematics* 7th edn (New York: Wiley)
[2] Ray Wylie C and Barrett L C 1985 *Advanced Engineering Mathematics* 5th edn (Singapore: McGraw-Hill)
[3] Gabor D 1946 *J. Inst. Elect. Eng. (London)* **93** 429–57
[4] Kaiser G 1994 *A Friendly Guide to Wavelets* (Boston, MA: Birkhäuser)
[5] Fourier J 1822 Théorie Analytique de la Chaleur *Œuvres de Fourier* ed G Darboux (1888) Tome Premiére (Paris: Gauthier-Villars)
[6] Tsallis C 1988 *J. Stat. Phys.* **52** 479–87
[7] Curado E M F and Tsallis C 1991 *J. Phys. A: Math. Gen.* **24** L69
   Curado E M F and Tsallis C 1991 *J. Phys. A: Math. Gen.* **24** 3187 (erratum)
   Curado E M F and Tsallis C 1992 *J. Phys. A: Math. Gen.* **25** 1019 (erratum)
[8] Abe S and Okamoto Y (ed) 2001 *Nonextensive Statistical Mechanics and its Applications (Lecture Notes in Physics)* (Berlin: Springer)
[9] Gell-Mann M and Tsallis C (ed) 2004 *Nonextensive Entropy—Interdisciplinary Applications* (New York: Oxford University Press)
[10] Alemany P A and Zanette D H 1994 *Phys. Rev.* E **49** R956–8
[11] Zanette D H and Alemany P A 1995 *Phys. Rev. Lett.* **75** 366–9
[12] Tsallis C, de Souza A M C and Maynard R 1995 Derivation of Lévy-type anomalous superdiffusion from generalized statistical mechanics *Lévy Flights and Related Topics in Physics* ed M F Shlesinger, G M Zaslavsky and U Frisch (Berlin: Springer) pp 269–89
[13] Zanette D H 1999 *Braz. J. Phys.* **29** 108–24
[14] Wilk G and Włodarczyk Z 2000 *Phys. Rev. Lett.* **84** 2770–3
[15] Tsallis C, Levy S V F, de Souza A M C and Maynard R 1996 *Phys. Rev. Lett.* **75** 3589–93
   Tsallis C, Levy S V F, de Souza A M C and Maynard R 1996 *Phys. Rev. Lett.* **77** 5442 (erratum)
[16] Prato D and Tsallis C 1999 *Phys. Rev.* E **60** 2398–401
[17] Plastino A R and Plastino A 1993 *Phys. Lett.* A **174** 384–6
[18] Hamity V H and Barraco D E 1996 *Phys. Rev. Lett.* **76** 4664–6
[19] Boghosian B M 1996 *Phys. Rev.* E **53** 4754–63
[20] Anteneodo C and Tsallis C 1997 *J. Mol. Liq.* **71** 255–67
[21] Boghosian B M 1999 *Braz. J. Phys.* **29** 91–107
[22] Arimitsu T and Arimitsu N 2000 *Phys. Rev.* E **61** 3237–40
[23] Arimitsu T and Arimitsu N 2000 *J. Phys. A: Math. Gen.* **33** L235–41
[24] Beck C 2000 *Physica* A **277** 115–23
[25] Beck C, Lewis G S and Swinney H L 2001 *Phys. Rev.* E **63** 035303(R)
[26] Tsallis C, Anjos J C and Borges E P 2003 *Phys. Lett.* A **310** 372–6
[27] Tsallis C and Borges E P 2003 Nonextensive statistical mechanics—applications to nuclear and high energy physics *Proc. 10th Int. Workshop on Multiparticle Production—Correlations and Fluctuations in QCD* ed N G Antoniou, F K Diakonos and C N Ktorides (Singapore: World Scientific) pp 326–43
[28] http://tsallis.cat.cbpf.br/biblio.htm
[29] Tsallis C, Mendes R S and Plastino A R 1998 *Physica* A **261** 534–54
[30] Beck C and Schlögl F 1995 *Thermodynamics of Chaotic Systems* (Cambridge: Cambridge University Press)

[31] Tsallis C 1994 *Quimica Nova* **17** 468–71
[32] Borges E P 1998 *J. Phys. A: Math. Gen.* **31** 5281–8
[33] dos Santos R J V 1997 *J. Math. Phys.* **38** 4104–7
[34] Kassel C 1995 *Quantum Groups* (New York: Springer)
[35] Gamero L G, Plastino A and Torres M E 1997 *Physica* A **246** 487–509
[36] Capurro A, Diambra L, Lorenzo D, Macadar O, Martin M T, Mostaccio C, Plastino A, Rofman E, Torres M E and Velluti J 1998 *Physica* A **257** 149–55
[37] Capurro A *et al* 1999 *Physica* A **265** 235–54
[38] Martin M T, Plastino A R and Plastino A 2000 *Physica* A **275** 262–71
[39] Tong S, Bezerianos A, Malhotra A, Zhu Y and Thakor N 2003 *Phys. Lett.* A **314** 354–61
[40] Daubechies I 1990 *IEEE Trans. Inf. Theory* **36** 961–1005
[41] Daubechies I 1992 *Ten Lectures on Wavelets (CBMS-NSF Regional Conference Series in Applied Mathematics vol 61)* (Philadelphia: SIAM)
[42] Hernández E and Weiss G 1996 *A First Course on Wavelets* (Boca Raton, FL: CRC Press)
[43] Tsallis C 2001 Nonextensive statistical mechanics and thermodynamics: historical back-ground and present status *Nonextensive Statistical Mechanics and its Applications (Lecture Notes in Physics)* ed S Abe and Y Okamoto (Berlin: Springer) p 8
[44] Borges E P 2004 *Physica* A **340** 95–101
[45] Suyari H and Tsukada M 2004 Law of error in Tsallis statistics *Preprint* cond-mat/0401540
[46] Suyari H 2004 Mathematical structure derived from the q-multinomial coefficient in Tsallis statistics *Preprint* cond-mat/0401546
[47] Suyari H 2004 q-Stirling's formula in Tsallis statistics *Preprint* cond-mat/0401541
[48] Gradshteyn I S and Ryzhik I M 1994 *Table of Integrals, Series, and Products* 5th edn, ed A Jeffrey (San Diego, CA: Academic)
[49] Morlet J, Arens G, Fourgeau I, and Giard D 1982 *Geophys.* **47** 203–36
[50] Grossmann A and Morlet J 1984 *SIAM J. Math. Anal.* **15** 723–36
[51] Grossmann A and Morlet J 1985 Decomposition of functions into wavelets of constant shape and related transforms *Mathematics and Physics (Lectures on Recent Results)* ed L Streit (Singapore: World Scientific)
[52] Temme N M 1993 Wavelets: first steps *Wavelets: An Elementary Treatment of Theory and Applications* ed T K Koornwinder (Singapore: World Scientific) 1–12
[53] Meyer Y 1990 *Ondelettes* (Paris: Hermann)
[54] Holschneider M 1995 *Wavelets, An Analysis Tool* (Oxford: Clarendon)
[55] Muzy J F, Bacry E and Arneodo A 1994 *Int. J. Bifurcation Chaos* **4** 245–302